Ecological Applications, 17(5), 2007, pp. 1379–1387

SOIL EROSION AND SIGNIFICANCE FOR CARBON FLUXES IN A MOUNTAINOUS MEDITERRANEAN-CLIMATE WATERSHED

S. V. Smith,[1,4] S. H. Bullock,[2] A. Hinojosa-Corona,[1] E. Franco-Vizcaíno,[2] M. Escoto-Rodríguez,[1] T. G. Kretzschmar,[1] L. M. Farfán,[3] and J. M. Salazar-Ceseña[2]

[1]*Departamento de Geología, Centro de Investigación Científica y de Educación Superior de Ensenada, Ensenada, Baja California 22860 Mexico*
[2]*Departamento de Biología de la Conservación, Centro de Investigación Científica y de Educación Superior de Ensenada, Ensenada, Baja California 22860 Mexico*
[3]*Unidad La Paz, Centro de Investigación Científica y de Educación Superior de Ensenada, La Paz, Baja California Sur 23050 Mexico*

Abstract. In topographically complex terrains, downslope movement of soil organic carbon (OC) can influence local carbon balance. The primary purpose of the present analysis is to compare the magnitude of OC displacement by erosion with ecosystem metabolism in such a complex terrain. Does erosion matter in this ecosystem carbon balance? We have used the Revised Universal Soil Loss Equation (RUSLE) erosion model to estimate lateral fluxes of OC in a watershed in northwestern Mexico. The watershed (4900 km^2) has an average slope of $10° \pm 9°$ (mean ± SD); 45% is >10°, and 3% is >30°. Land cover is primarily shrublands (69%) and agricultural lands (22%).

Estimated bulk soil erosion averages 1350 $Mg \cdot km^{-2} \cdot yr^{-1}$. We estimate that there is insignificant erosion on slopes <2° and that 20% of the area can be considered depositional. Estimated OC erosion rates are 10 $Mg \cdot km^{-2} \cdot yr^{-1}$ for areas steeper than 2°. Over the entire area, erosion is ~50% higher on shrublands than on agricultural lands, but within slope classes, erosion rates are more rapid on agricultural areas.

For the whole system, estimated OC erosion is ~2% of net primary production (NPP), increasing in high-slope areas to ~3% of NPP. Deposition of eroded OC in low-slope areas is ~10% of low-slope NPP. Soil OC movement from erosional slopes to alluvial fans alters the mosaic of OC metabolism and storage across the landscape.

Key words: erosion; lateral flux; local carbon balance; metabolism; Mexico; primary production; Revised Universal Soil Loss Equation (RUSLE); vertical flux.

Introduction

Lateral transfers of organic carbon (OC) are often considered to be small in local, regional, and global analyses of carbon cycling (Randerson et al. 2002). In the global context, net primary production (NPP) on land totals $\sim 60 \times 10^9$ Mg C/yr, while OC transport from land to the ocean is $\sim 0.5 \times 10^9$ Mg C/yr (Schlesinger and Melack 1981, Smith and Hollibaugh 1993, Schimel 1995), ~1% of terrestrial NPP. However, OC erosion is at least three times the OC transfer from land to ocean by rivers (Smith et al. 2001). This difference between OC erosion and land–ocean transport approximates the magnitude of the "missing carbon sink" assumed to reside somewhere on land ($\sim 2 \times 10^9$ Mg C/yr; Houghton 2003). The fates of the OC erosion products that do not reach the ocean are matters of intense debate (e.g., Schlesinger 1995, Stallard 1998, Harden et al. 1999, Smith et al. 2001, 2005, Liu et al. 2003, Lal et al. 2004). The significance of lateral fluxes becomes especially apparent in relation to net ecosystem production (NEP), typically a small fraction of NPP.

Erosional relocation of carbon may be particularly important in topographically heterogeneous environments and could represent quantitatively significant components of local carbon balance. At a minimum, relocation of OC might alter net metabolism in subsets of a watershed without altering net metabolism of the total watershed. Additionally, oxidation rates of OC may differ between upland erosional sites and downslope depositional sites, altering landscape total carbon storage.

The underlying hypothesis of this paper is that OC erosion, lateral translocation, and deposition, all within the boundaries of a watershed, can be quantitatively significant in local OC balances in a topographically complex landscape. We examine this argument by estimating bulk soil and soil OC erosion and then comparing estimated OC erosion with estimates of metabolism in a mountainous Mediterranean-climate regime.

Study System

The Todos Santos Watershed covers 4900 km^2 (Figs. 1, 2) in northwestern Baja California, Mexico. Elevation

Manuscript received 13 April 2006; revised and accepted 11 December 2006. Corresponding Editor: B. A. Hungate.
[4] E-mail: svsmith@cicese.mx

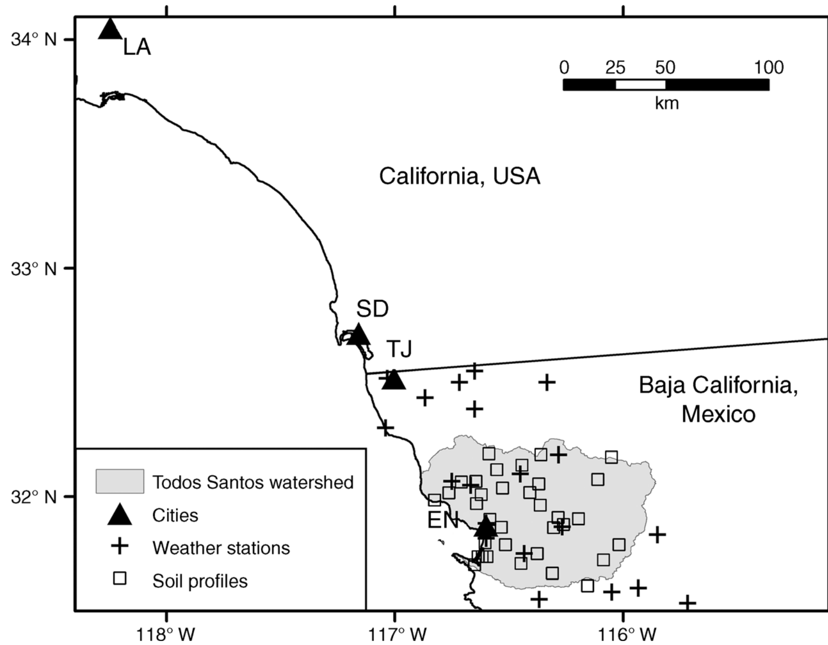

FIG. 1. Index map of Baja California, Mexico, showing location of the Todos Santos Watershed. The cities of Ensenada (EN), Tijuana (TJ), San Diego (SD), and Los Angeles (LA) are identified. The figure also shows the locations of weather stations in or near the watershed, used to estimate precipitation and air temperature and the soil profiles used to estimate properties of soil types.

ranges between sea level and 1876 m. The area is topographically complex, with steep slopes, large intermountain alluvial valleys, alluvial deposits in streambeds, and an alluvial coastal plain. The climate is Mediterranean, with cool, moist winters and warm, dry summers. Mean precipitation is ~315 mm/yr (~85% between November and April). There is no significant perennial stream flow. Mean annual temperature is ~16°C (±6°C variation for watershed-averaged monthly means).

Much of the coastal plain and middle-elevation alluvial area was cleared for urban and agricultural development, beginning in the late 19th century. Coastal scrub (drought-deciduous and evergreen shrubs and succulents; Zippin and Vanderwier 1994) occurs along a belt to ~50 km inland and/or 500 m elevation. Chaparral (evergreen sclerophyllous shrubs) covers the upper slopes of coastal and inland hills (Minnich and Franco-Vizcaíno 1997). These two types of native scrubland intergrade with one another and with introduced annual plants in complex patterns depending upon elevation, aspect, fire history, and other factors (Peinado et al. 1995). A plateau at the upper limit of the watershed hosts pine forest and mountain meadows.

Materials and Methods

Erosion

We used the Revised Universal Soil Loss Equation (RUSLE, Renard et al. 1996; a revision of the USLE, Wischmeier and Smith 1978). This model considers erosive energy of precipitation, soil erodibility, local topography, and land cover to estimate erosion. While the equation can be solved for any prescribed time span, results based on long-term precipitation history are considered by the above authors and others to be quantitatively the most robust.

We used GIS (ArcView 8.3, including Spatial Analyst; Environmental Systems Research Institute, Redlands, California, USA) to examine spatial variations in erosion, using elevation data at a 30-m grid scale, a total of ~5.5×10^6 grid cells within the study area. Digital soil and land cover data are available as ArcView shape files.

The formulation for RUSLE is

$$A = R \times K \times L \times S \times C \times P. \quad (1)$$

A methodological summary for estimating each term follows, with more details in the Appendix.

A is soil loss from sheet and rill erosion, reported here in megagrams per square kilometer per year, numerically equivalent to grams per square meter per year, for easy comparison with metabolic rates.

R (in megajoule-millimeters per square kilometer per hour per year), the rainfall-runoff factor, represents erosional energy; it is estimated here by two methods. The first (preferred) method (Renard et. al. 1996) uses 10-min precipitation data to calculate the intensity of individual rainfall events. Data were available for the period October 1999–June 2005 from a weather station in Ensenada (Presa Emilio López Zamora, Servicio Meteorológico Nacional, SMN; *available online*).[5] Be-

[5] ⟨http://smn.cna.gob.mx/productos/emas/emas.html⟩

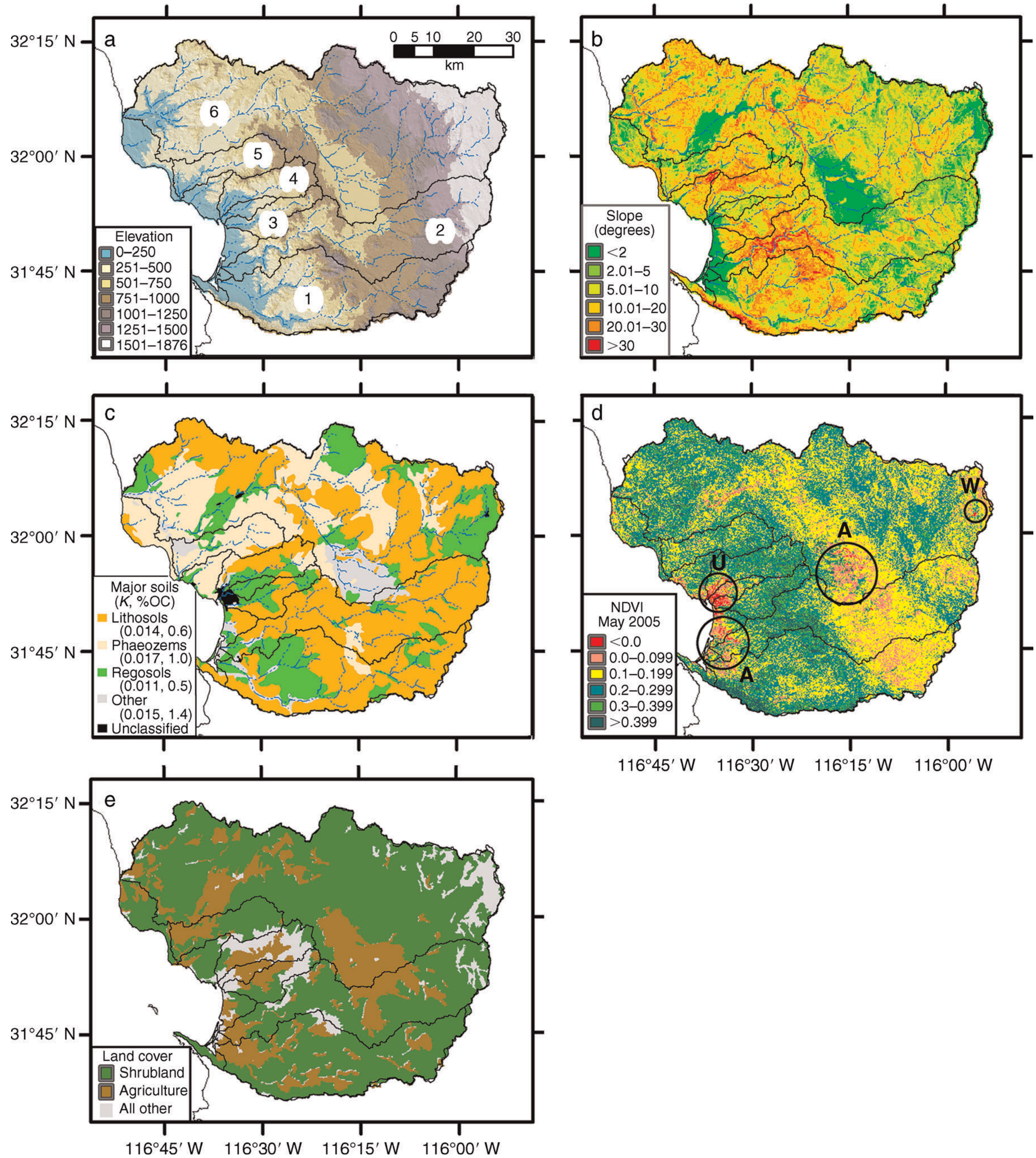

FIG. 2. (a) Elevation of the Todos Santos Watershed, based on a 30-m digital elevation model (DEM). The six major catchments in the watershed are outlined. Numbers on the catchments correspond to the numbers in Table 1. Stream courses (in blue) are calculated from the DEM and include all streams with catchment areas $\geq$10 km^2. (b) Slope, based on DEM data in (a). (c) Major soil types. The values in parentheses represent *K*, the soil erodibility factor, and %OC, the percentage of organic carbon, respectively. (d) Normalized difference vegetation index (NDVI) for May 2005. Both the urban area of Ensenada (U) and the most prominent freshwater area (Laguna Hanson, W) are labeled and show low NDVI. Two of the agricultural areas (A, south and northeast of Ensenada) are characterized by relatively coarse, largely rectangular patches (fields) of high and low NDVI. (e) Distribution of shrubland, mixed agricultural cover, and other land cover.

cause such high-resolution precipitation data are uncommon and a data record of at least 22 years is recommended to characterize variations in precipitation intensity, *R* was also calculated from annual precipitation data from the regression relationship of Renard and Freimund (1994). A 100-year record for Ensenada is available, as are precipitation data for $\geq$10 years between 1960 and 1990 at 22 additional stations within

TABLE 1. Major catchments of the Todos Santos watershed in northwestern Baja California, Mexico.

Catchment	Area (km^2)	Maximum elevation (m)	Slope (°)	Percentage with slope <2°
1) Maneadero	844	1660	12.1 ± 9.6	16.4
2) San Carlos	845	1863	10.3 ± 9.4	17.3
3) El Gallo	129	1113	13.4 ± 8.8	9.5
4) Ensenada	177	1140	13.8 ± 9.1	9.1
5) San Miguel	210	1336	12.3 ± 8.6	26.7
6) La Misión	2398	1876	9.3 ± 8.1	20.7
Aggregate <100 km^2	321	780	8.6 ± 4.4	26.1
Total	4924	1876	10.3 ± 8.9	18.7

Notes: Catchment numbers correspond to the numbered regions on Fig. 2a. Values for slope are means ± SD. The slope break of 2° approximates the break between steep, erosional areas and flat, depositional areas.

or near the watershed (Comisión Nacional del Agua; *available online*)[6] (Fig. 1). Solution of the Renard and Freimund equation, using both annual time steps of the long-term record and the individual station average data, gives insight about interannual and spatial variation of R.

K (in megagram-hours per megajoule per millimeter) is the soil erodibility factor, the soil tendency to erode. We estimated K based on its empirical relationship with soil texture (Renard et al. 1996), using A-horizon data from 34 soil profiles in or immediately adjacent to the study area (Instituto Nacional de Estadística Geografía e Informática [INEGI] 2004) and mapped by INEGI (Figs. 1, 2c).

The units for R and K determine the units for A. Other terms in Eq. 1 are dimensionless ratios that scale field erosion estimates relative to experimental conditions under which erosion has been measured.

L and S are topographic factors typically combined into the LS factor. L scales the distance (length) of upstream flow accumulation at any field location to the length of the standard plot used for experimental erosion measurements (22.13 m), with a maximum effective slope length of ~150 m. S scales the steepness at the field site to the slope of the experimental plots (9%; 5.1°). Detailed procedures for calculating LS using GIS are presented in the Appendix. Data used for topographic analyses were INEGI 1 arc-second digital elevation model (DEM) data, resampled to a 30-m Universal Tranverse Mercator (UTM) grid (Snyder 1984; INEGI data, *available online*).[7]

C is the cover factor. Soils that are constantly tilled or otherwise disturbed have maximum potential for erosion ($C = 1$). Any kind of cover shields soil, impedes erosion, and reduces C. Soil that has not been recently disturbed "crusts over" and has a nominal C of 0.45. Live or dead vegetation and rocks reduce C.

Many GIS-based estimates of C use a remotely estimated normalized difference vegetation index (NDVI) (Sabins 1997) to derive a geospatially distributed estimate for C. Live plants typically exhibit NDVI values above 0.4, while dry vegetation, bare soil, rock, and water have NDVI $\leq$ 0.0. Data from an image (5 May 2005) from the Landsat Thematic Mapper sensor were used to derive local NDVI (*available online*).[8] We used a modification of the equation by de Jong and colleagues (de Jong 1994; S. M. de Jong, *unpublished manuscript* [1994 technical report] and de Jong et al. 1998 as cited in van der Knijff et al. 1999) to estimate C (Appendix).

In order to relate C to general land cover type, we used digital data from the Comisión Nacional Forestal (CONAFOR; *available online*).[9] These data show several land cover classes ("chaparral" is broadly interpreted in the data, and "coastal scrub" very narrowly); eventually these were collapsed to shrubland, agriculture, and all other cover.

The last term in Eq. 1 is P, the support practice factor. This term is an estimate of the efficiency of management practices employed to ameliorate erosion. Few such practices are applied locally, so a constant value of 1.0 was applied.

In summary, LS and C (Eq. 1) provide estimates of high-resolution spatial variation across the area. K provides much lower resolution of spatial variation, based on the soils map. R is treated as spatially constant. Because R is both spatially and temporally variable, we will explore the potential significance of this treatment assumption. P is treated as constant.

RESULTS

Physiography

Three catchments occupy ~83% of the watershed (Fig. 2, Table 1). Three smaller catchments occupy another 11%, and a coastal strip with individual catchments <100 km^2 constitutes the remainder. Mean elevation is 785 m.

Watershed slopes are 10° ± 9° (mean ± SD). Approximately 3% of the area is steeper than 30°. Slopes between 10° and 20° account for 27% of the area, and alluvial areas with slopes <2° occupy ~19% (Fig.

[6] ⟨http://smn.cna.gob.mx/productos/normales/estacion/normales.html⟩

[7] ⟨http://www.inegi.gob.mx⟩

[8] ⟨http://edc.usgs.gov/guides/landsat_tm.html⟩

[9] ⟨http://www.conafor.gob.mx/⟩

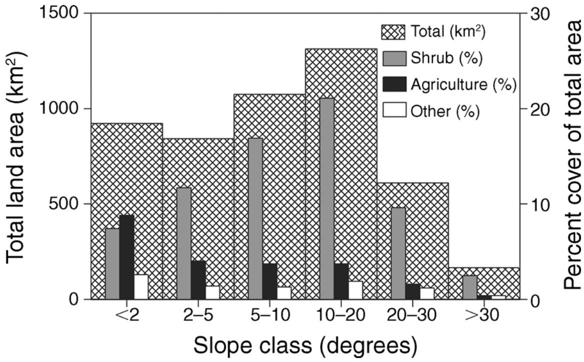

FIG. 3. Histogram showing the relationship between major land cover types and slope.

2b). There are two large, mid-altitude alluvial areas ($\sim$700, 300 m) and a coastal plain (<50 m) consisting of coalescing alluvial fans. All include significant agricultural activities, and the coastal plain includes most of the Ensenada urban area (Fig. 2b–d). In addition to these large alluvial regions, there are many smaller, more dispersed depositional areas. The other major depositional site is a water reservoir that intercepts sediments from $\sim$150 km^2 (90%) of the Ensenada catchment (Table 1).

Land cover and its relationship to physiography

Chaparral and coastal scrub shrublands (pure and mixed stands; stands with invasive grasses; grouped as "shrubland") occupy 69% of the total watershed, while agricultural areas (irrigated and non-irrigated plant agricultural land and grazing areas) occupy 22%; agricultural cover may be slightly overestimated by inclusion of some early post-burn or naturally sparse shrublands. Other cover (evergreen, mixed woodlands, urban, etc.) occupies 9% (Fig. 2e).

Land cover varies with slope (Fig. 3). For areas <2°, shrubland and agriculture are about equal in area covered, but with significant other cover (in this case, predominantly urban). Shrubland dominates on higher slopes. Other cover at slopes >5° largely consists of deciduous woodlands at lower elevations, evergreens at higher elevations, with some penetration of both agricultural and urban areas to higher slopes. Shrubland occupies average slopes of 11° $\pm$ 9°; agriculture, 7° $\pm$ 8°; other, 10° $\pm$ 13° (Fig. 3).

Erosion

Estimated bulk erosion averages 1353 $\pm$ 1551 $\mathrm{Mg \cdot km^{-2} \cdot yr^{-1}}$ (Fig. 4). Erosion is constrained to values ≥ 0, so the large standard deviation reflects a nonnormal distribution of the data. $\mathrm{Log_{10}(erosion + 1)}$ averages 2.79

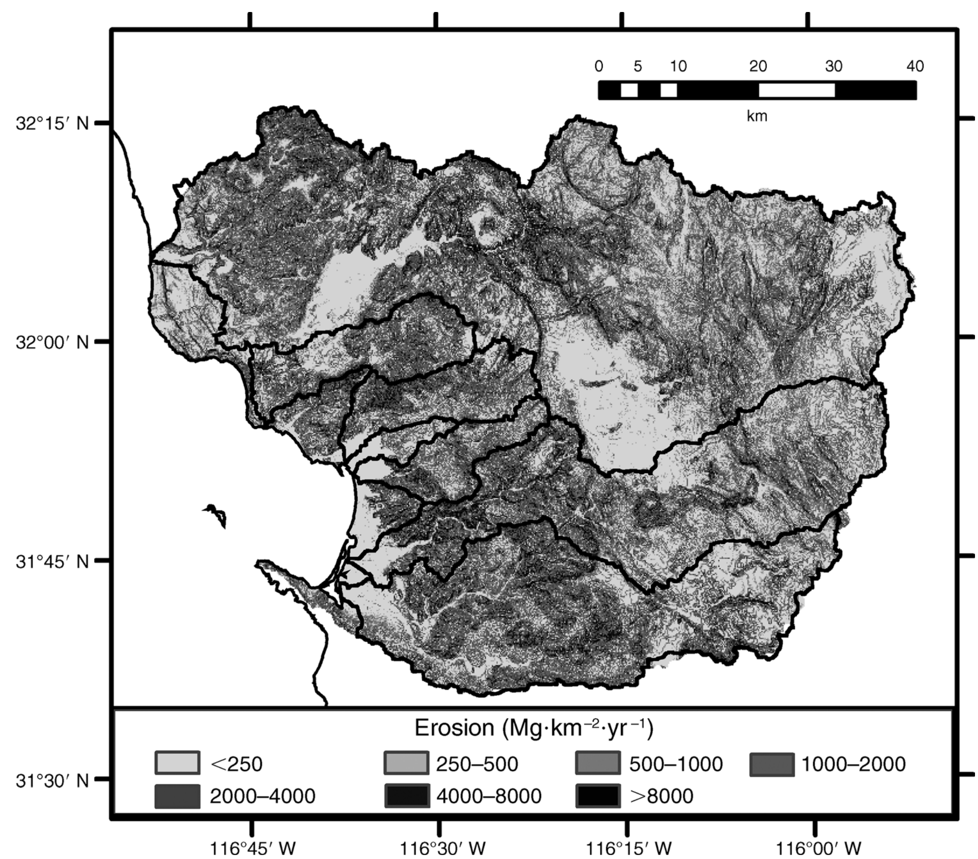

FIG. 4. Soil erosion rates. These values were multiplied by 0.006 to estimate soil organic carbon erosion rates.

TABLE 2. Model 2 linear regression equations and coefficients of determination for the Revised Universal Soil Loss Equation (RUSLE) erosion estimates within land cover types as functions of topographic slope.

Land cover type	No. pixels	Regression slope (b)	Y intercept, a_Y	X intercept, a_X	r^2
Shrubland	3 783 179	176 ± 0.1	−517 ± 1.0	2.9 ± 0.01	0.52
Agriculture	1 209 049	188 ± 0.3	−278 ± 1.6	1.5 ± 0.01	0.62
Other	474 360	144 ± 0.4	−419 ± 2.4	2.9 ± 0.02	0.54
Total	5 468 588	175 ± 0.1	−452 ± 0.9	2.6 ± 0.00	0.53

Notes: The mean ± SE for each coefficient (regression slopes and intercepts) is calculated according to propagation analysis of independent errors. The environmental significance of the X intercepts is discussed in *Results: Erosion*.

± 0.68, with a near-normal distribution, skewed towards low values. Approximately 13% of the area has erosion <100 Mg·km^{-2}·yr^{-1}, and 45% has erosion >1000 Mg·km^{-2}·yr^{-1}.

Erosion is strongly related to topographic slope (Table 2). Calculated erosion on shrubland (1505 ± 1550 Mg·km^{-2}·yr^{-1}) is about 50% higher than on agricultural land (1010 ± 1520 Mg·km^{-2}·yr^{-1}) or other cover (1014 ± 1432 Mg·km^{-2}·yr^{-1}), but high shrubland erosion is partially a consequence of anthropogenic displacement of shrubs from low slopes. Erosion increases more sharply with slope for agricultural lands than for shrublands (higher regression slope and a less negative Y intercept).

The X intercept represents the topographic slope below which the linear extrapolation of erosion is negative. Because calculated erosion must be positive or equal to zero, this intercept is interpreted to represent the topographic slope below which erosion apparently does not occur. This threshold lies at slopes between 1.5° and 2.9°; we use a nominal value of 2° to separate erosional and depositional regimes. Agriculture shows the lowest slope threshold for erosion, and agricultural lands at any slope apparently erode ~300 Mg·km^{-2}·yr^{-1} more rapidly than shrublands. Across the entire watershed, erosion products derived from ~80% of the landscape are carried downhill until they are intercepted and deposited within ~20% of the area (Table 1).

Soil OC erosion is simply treated as 0.6% of bulk erosion across the watershed, because the available data on soil OC are too sparse to assert any differences among soil types or to allow geospatial pedometric modeling.

DISCUSSION

Redistribution of materials by erosion within the system

The Todos Santos Watershed is an instructive example of the potential importance of downslope lateral fluxes of materials in the carbon balance of a topographically complex region. This mountainous regime shows wide slope-dependent variation in bulk erosion rates, varying from <100 to >3000 Mg·km^{-2}·yr^{-1} (<1–18 Mg OC·km^{-2}·yr^{-1}). Eroding material on slopes moves downhill until it encounters flats. The estimated rate of bulk soil displacement from areas with >2° slope to areas with <2° slope is 1650 Mg·km^{-2}·yr^{-1}, and OC displacement is 10 Mg·km^{-2}·yr^{-1}. This underestimates OC displacement, because it is based on A-horizon soil OC, while eroding material in the surficial (O) horizon has higher OC. Although the erosion products on the slopes do not immediately reach the flats, the processes treated by RUSLE estimate long-term average flux. We further estimate that only a small fraction (~0) of the material displaced from the slopes moves beyond the intercepting flats except during extreme runoff events.

Processes controlling erosion

Spatial variation of erosion in this mountainous terrain appears to be dominated by slope. Agriculture apparently increases erosion, so erosion will increase as agriculture expands upslope. Other factors affecting spatial and temporal variations in flux also merit consideration.

The RUSLE model considers only raindrop splash to break soil particles loose and then sheet and rill erosion to displace the materials. Other forms of erosion occur in the region, including various forms of mass slippage (e.g., slumps, landslides). Campbell (1975) observed in southern California that soil slippage most commonly occurs on slopes >27° (~5% of the Todos Santos watershed area). Adding soil slippage, for which we have no local estimates, to the estimates for sheet and rill erosion would further emphasize the importance of erosion.

Spatial resolution of K is low, and higher resolution would influence detailed distribution of estimated erosion. However, variations in parent materials and weathering seem to be adequately represented, so average K may not be greatly changed by further sampling. By contrast, geographic and vertical resolution of soil OC would alter (raise) OC erosion estimates.

This watershed is dynamic with respect to variation of land cover. Fire is a locally important process. Each dry season sees a mosaic of fires across the watershed. These usually affect ~1% of the watershed each year, with the majority of individual burns <1 km^2 (Comisión Nacional Forestal; see footnote 9). However, the largest fires have exceeded 100 km^2. Besides removing vegetation (raising C), studies elsewhere have demonstrated that fires can elevate the hydrophobic characteristics of underlying soil (raising K) (DeBano 2000). Thus, fires can drastically alter local erosion in the ensuing wet

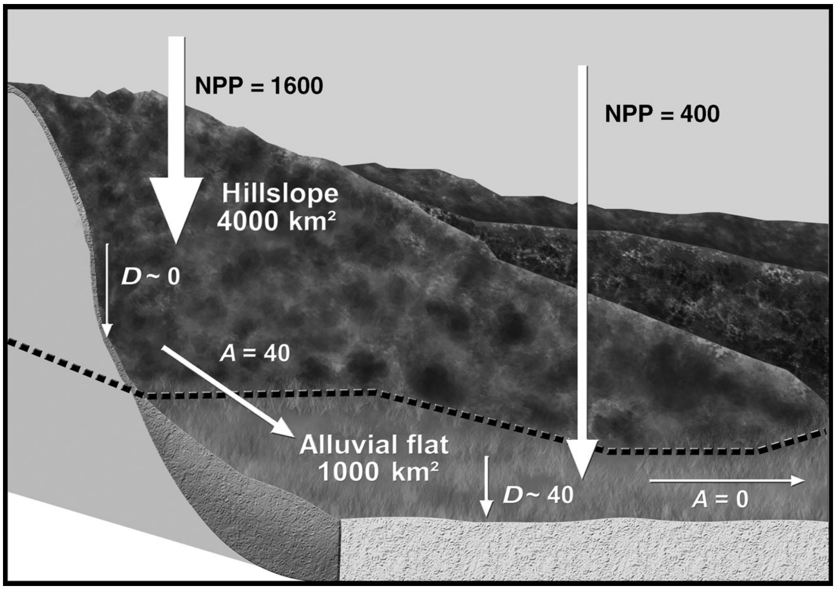

FIG. 5. Schematic diagram illustrating the relative importance of erosion across the landscape. Hillslope erosion (A) is assumed to accumulate as deposition in alluvial flat areas (D). Export of eroded materials from the alluvial areas is assumed to be 0. Net primary production (NPP) of hillslope and alluvial areas is assumed to be constant (400 $g \cdot m^{-2} \cdot yr^{-1}$). Total organic carbon (OC) depositional fluxes in each subsystem are only approximate, because the diagram does not include net ecosystem production (NEP). Organic carbon fluxes on the diagram are in Gg/yr.

season (Rice 1982, Wohlgemuth 1986, Florsheim et al. 1991), followed by some years before recovery to preburn conditions. Loss of cover and increased hydrophobic soil will also exacerbate landslides.

Local land use is rapidly changing cover, with overgrazing or conversion of shrublands, abandonment of agricultural lands, and invasion by introduced species, especially annual grasses. Moreover, northwestern Baja California has experienced accelerating demographic and economic growth during the last half century as people have immigrated and urbanized the region. Construction sites without erosion mediation represent a cover disturbance analogous to soil tilling (Wischmeier and Smith 1978). These details would not influence the essential conclusion of our analysis, but such modifications are important details in local erosion and relocation of erosion products and are amenable to management.

Better resolution of R would alter estimated erosion. Based on both the limited available local weather data and documented trends in southern California, we expect that more highly resolved estimates of precipitation would show either an elevation gradient or some other geographically consistent pattern. The rainfall-runoff factor is not a simple linear function of total precipitation but includes intensity, and it is estimated to increase as the 1.61 power of annual precipitation (Renard and Freimund 1994). This implies a fourfold variation in R among weather stations across the watershed, based on average precipitation, and an 18-fold interannual variation in R based on the long-term Ensenada data.

Metabolic and non-metabolic components of ecosystem carbon balance

Placing the estimate of lateral flux of OC into the context of ecosystem carbon balance requires consideration of ecosystem metabolism (see Appendix for more details). There are no ground-based NPP estimates for the study area, but models using climate data and moderate-resolution imaging spectroradiometer (MODIS)-derived NDVI time series suggest that NPP ranges between ~250 (Lieth 1975) and 500 $Mg \cdot km^{-2} \cdot yr^{-1}$ (MOD17A3; Heinsch et al. 2003), without demonstrable differences between slopes and flats. The NPP estimates from ground-based studies in shrublands in southern California demonstrate some patterning by slope aspect, species, and time since fire (Kittredge 1955, Mooney et al. 1977, Kummerow et al. 1981, Miller 1981, Oechel and Lawrence 1981, Gray 1982) but cannot presently be reconciled into a regional geospatial model. The weight of field evidence does suggest that local NPP is substantially less than the MODIS estimates (see also Turner et al. 2005). We use a nominal NPP estimate of 400 $Mg \cdot km^{-2} \cdot yr^{-1}$. Bounds on heterotrophic respiration are even more poorly constrained. Model results from climatic data (Raich et al. 2002) suggest that R_s (heterotrophic plus autotrophic root R) is in the range of NPP. That being the case, the erosional export of 10 $Mg \cdot km^{-2} \cdot yr^{-1}$ from slopes to flats is likely to be significant in the local carbon balance.

Despite the assertion by Randerson et al. (2002) that NEP must be considered as net accumulation (i.e., net carbon accumulation [dC/dt] = NEP), we prefer to retain

the concept as net organismic metabolism while recognizing the principles of mass balance. The following equation recognizes that total system mass balance (i.e., net carbon accumulation or loss, dC/dt) approximates, but does not equal, NEP:

$$dC/dt = \mathrm{NEP} + \sum F_o \qquad (2)$$

where NEP is defined metabolically in terms of either gross primary production (GPP) and ecosystem respiration (R_e) or NPP and heterotrophic respiration (R_h). This definition moves the sum of non-metabolic processes (ΣF_o) from inside to outside the definition of NEP. ΣF_o is typically a small fraction of NPP, but NEP is, likewise, a small fraction of NPP. Consistent with one historical precedent for the definition of NEP (Randerson et al. 2002), Eq. 2 accentuates the comparison between metabolic and non-metabolic components of ecosystem carbon balance.

The utility of defining NEP according to Eq. 2 can be illustrated with a schematic diagram of NPP, erosional displacement, and deposition within the Todos Santos watershed (Fig. 5; fluxes in gigagrams per year). We use an average NPP of 400 $Mg \cdot km^{-2} \cdot yr^{-1}$ across an area of 5000 km^2, with 80% hillslope and 20% alluvial flat. From Randerson et al. (2002), it can be assumed that dC/dt is ~10% of NPP. By comparison, displaced OC removed from the slopes and deposited on the flats represents ~3% of NPP on slopes, but ~10% of NPP on the flats. Maintaining the definition of NEP as presented in Eq. 2 distinguishes the roles of metabolic and non-metabolic components of ecosystem carbon balance.

Conclusions

Balancing carbon budgets at local to global scales remains challenging. Topographically complex ecosystems provide insight into this problem. When erosional displacement from high-slope to low-slope areas occurs, the displaced material may represent a significant fraction of NPP. Displacement of reactive OC has the potential consequence of spatially distorting the landscape pattern of NPP and R_h. In the system we have examined, the low-slope deposition of OC is on the order of 10% of NPP. If the underlying values for R_h within the subsystems differ, the effect may also be a system-wide alteration of metabolically defined NEP. If we accept that dC/dt is also of the order of 10% of NPP and can be either positive or negative, then splitting carbon storage into its metabolic and non-metabolic components helps to characterize the processes accounting for carbon storage within the ecosystem.

Acknowledgments

This research has been supported by SEP-CONACYT Project Number V43422-F and by CICESE internal funds. We thank Michel Rosengaus-Moshinsky (SMN/CNA) and Santiago Higareda-Cervera (CICESE) for providing meteorological data, and Montserrat Porredon for help with the artwork.

Literature Cited

Campbell, R. H. 1975. Soil slips, debris flows, and rainstorms in the Santa Monica Mountains and vicinity, southern California. United States Geological Survey (USGS) Professional Paper 851. USGS, Washington, D.C., USA.

DeBano, L. F. 2000. The role of fire and soil heating on water repellency in wildland environments: a review. Journal of Hydrology 231–232:195–206.

de Jong, S. M. 1994. Derivation of vegetative variables from a Landsat TM image for modeling soil erosion. Earth Surface Processes and Landforms 19:165–178.

Florsheim, J. L., E. A. Keller, and D. W. Best. 1991. Fluvial sediment transport in response to moderate storm flows following chaparral wildfire, Ventura County, southern California. Geological Society of America Bulletin 103:504–511.

Gray, J. T. 1982. Community structure and productivity in *Ceanothus* chaparral and coastal sage scrub of southern California. Ecological Monographs 52:414–434.

Harden, J. W., J. M. Sharpe, W. J. Parton, D. S. Ojima, T. L. Fries, T. G. Huntington, and S. M. Dabney. 1999. Dynamic replacement and loss of soil carbon on eroding cropland. Global Biogeochemical Cycles 13:885–901.

Heinsch, F. A., et al. 2003. User's guide: GPP and NPP (MOD17A2/A3) products NASA MODIS land algorithm. Version 2.0. ⟨www.ntsg.umt.edu/modis/MOD17UsersGuide.pdf⟩

Houghton, R. A. 2003. Why are estimates of the terrestrial carbon balance so different? Global Change Biology 9:500–509.

INEGI [Instituto Nacional de Estadística, Geografía e Informática]. 2004. Información nacional sobre perfiles de suelo. Version 1.2. Instituto Nacional de Estadística, Geografía e Informática, Aguascalientes, Mexico.

Kittredge, J. 1955. Litter and forest floor of the chaparral in parts of San Dimas Experimental Forest, California. Hilgardia 23:563–593.

Kummerow, J., G. Montenegro, and D. Krause. 1981. Biomass, phenology and growth. Pages 69–96 *in* P. C. Miller, editor. Resource use by chaparral and matorral: a comparison of vegetation function in two mediterranean type ecosystems. Springer-Verlag, New York, New York, USA.

Lal, R., M. Griffin, J. Apt, L. Lave, and M. G. Morgan. 2004. Managing soil carbon. Science 304:393.

Lieth, H. 1975. Modeling the primary productivity of the world. Pages 237–263 *in* H. Lieth and R. H. Whittaker, editors. Primary productivity of the biosphere. Springer-Verlag, New York, New York, USA.

Liu, S., N. Bliss, E. Sundquist, and T. G. Huntington. 2003. Modeling carbon dynamics in vegetation and soil under the impact of soil erosion and deposition. Global Biogeochemical Cycles 17:1074. [doi:10.1029/2002GB002010.]

Miller, P. C. 1981. Similarities and limitations of resource utilization in Mediterranean type ecosystems. Pages 369–407 *in* P. C. Miller, editor. Resource use by chaparral and matorral: a comparison of vegetation function in two mediterranean type ecosystems. Springer-Verlag, New York, New York, USA.

Minnich, R. A., and E. Franco Vizcaíno. 1997. Mediterranean vegetation of Baja California. Fremontia 25:3–12.

Mooney, H. A., J. Kummerow, A. W. Johnson, D. J. Parsons, S. C. Keeley, A. Hoffmann, R. I. Hays, J. Gilberto, and C. Chu. 1977. The producers—their resources and adaptive responses. Pages 85–143 *in* H. A. Mooney, editor. Convergent evolution in Chile and California: Mediterranean climate ecosystems. Dowden, Hutchinson and Ross, Stroudsburg, Pennsylvania, USA.

Oechel, W. C., and W. Lawrence. 1981. Carbon allocation and utilization. Pages 185–235 *in* P. C. Miller, editor. Resource use by chaparral and matorral: a comparison of vegetation

function in two mediterranean type ecosystems. Springer-Verlag, New York, New York, USA.

Peinado, M., F. Alcaraz, J. L. Aguirre, J. Delgadillo, and J. Aguado. 1995. Shrubland formations and associations in Mediterranean-desert transitional zones of northwestern Baja California. Vegetatio 117:165–179.

Raich, J. W., C. S. Potter, and D. Bhagawati. 2002. Interannual variability in global soil respiration, 1980–94. Global Change Biology 8:800–812.

Randerson, J. T., F. S. Chapin, III, J. W. Harden, J. C. Neff, and M. E. Harmon. 2002. Net ecosystem production: a comprehensive measure of net carbon accumulation by ecosystems. Ecological Applications 12:937–947.

Renard, K. G., G. R. Foster, G. A. Weesies, D. K. McCool, and D. C. Yoder, coordinators. 1996. Predicting soil erosion by water: a guide to conservation planning with the Revised Universal Soil Loss Equation (RUSLE). USDA Handbook Number 703. USDA, Washington, D.C., USA.

Renard, K. G., and J. R. Freimund. 1994. Using monthly precipitation data to estimate the R-factor in the revised USLE. Journal of Hydrology 157:287–306.

Rice, R. M. 1982. Sedimentation in the chaparral: How do you handle unusual events? Pages 39–46 *in* F. J. Swanson, R. J. Janda, T. Dunne, and D. N. Swanston, editors. Sediment budgets and routing in forested drainage basins. General Technical Report PNW-141. USDA Forest Service, Portland, Oregon, USA.

Sabins, F. F. 1997. Remote sensing: principles and interpretation. Freeman, New York, New York, USA.

Schimel, D. S. 1995. Terrestrial ecosystems and the carbon cycle. Global Change Biology 1:77–91.

Schlesinger, W. H. 1995. Soil respiration and changes in soil carbon stocks. Pages 159–168 *in* G. M. Woodwell and F. T. Mackenzie, editors. Biotic feedbacks in the global climatic system: Will the warming feed the warming? Oxford Press, New York, New York, USA.

Schlesinger, W. H., and J. M. Melack. 1981. Transport of organic carbon in the world's rivers. Tellus 33:172–187.

Smith, S. V., and J. T. Hollibaugh. 1993. Coastal metabolism and the oceanic organic carbon balance. Reviews of Geophysics 31:75–89.

Smith, S. V., W. H. Renwick, R. W. Buddemeier, and C. J. Crossland. 2001. Budgets of soil erosion and deposition for sediments and sedimentary organic carbon across the conterminous United States. Global Biogeochemical Cycles 15:697–707.

Smith, S. V., R. O. Sleezer, W. H. Renwick, and R. W. Buddemeier. 2005. Fates of eroded soil organic carbon: Mississippi Basin case study. Ecological Applications 15: 1929–1940.

Snyder, J. P. 1984. Map projections used by the U.S. Geological Survey. U.S. Government Printing Office, Washington, D.C., USA.

Stallard, R. F. 1998. Terrestrial sedimentation and the carbon cycle: coupling weathering and erosion to the carbon cycle. Global Biogeochemical Cycles 12:231–257.

Turner, D. P., et al. 2005. Site-level evaluation of satellite-based global terrestrial gross primary production and net primary production monitoring. Global Change Biology 11:666–684.

Van der Knijff, J. M., R. J. A. Jones, and L. Montanarella. 1999. Soil erosion risk assessment in Italy. European Soil Bureau (European Commission) publication number EUR 19022EN. European Soil Bureau, Luxembourg.

Wischmeier, W. H., and D. D. Smith. 1978. Predicting rainfall erosion losses: a guide to conservation planning. USDA Handbook Number 537. USDA, Washington, D.C., USA.

Wohlgemuth, P. M. 1986. Spatial and temporal distribution of surface sediment transport in southern California steeplands. Pages 29–32 *in* J. J. DeVries, editor. Proceedings of the chaparral ecosystems research conference. Report 62. California Water Resources Center, Davis, California, USA.

Zippin, D. B., and J. M. Vanderwier. 1994. Scrub community descriptions of the Baja California peninsula, Mexico. Madroño 41:85–119.

APPENDIX

A discussion of parameter estimation for the RUSLE model, including detailed discussion of *C* derivation (*Ecological Archives* A017-052-A1).